A Comparative Femtosecond Coherence Study of the Unligated Monomeric Hemeproteins Myoglobin and Leghemoglobin

M. Halder,[†] K. Das,[†] P. K. Chowdhury,[†] S. Kundu,[‡] M. S. Hargrove,[‡] and J. W. Petrich*[,†]

Department of Chemistry and Department of Biochemistry, Biophysics, and Molecular Biology, Iowa State University, Ames, Iowa 50011

Received: March 31, 2003; In Final Form: June 30, 2003

Impulsive optical excitation has been performed on wild type, unligated leghemoglobin for the first time to compare the induced vibrational coherence with that observed in myoglobin. Both proteins were excited at the Soret maxima and probed at red and blue edges of the Soret band. The resulting kinetic traces were modulated by low-frequency vibrations. Leghemoglobin shows a decrease in vibrational amplitude compared with myoglobin. The possible cause for the amplitude differences is discussed in terms of contributions from both ground- and excited-state vibrational coherences and ground-state heterogeneity.

Introduction

Impulsive photoexcitation with ultrashort laser pulses is becoming a key tool in modern applications of ultrafast spectroscopy to chemical dynamics.[1] A laser pulse that is shorter than the time required for the constituent nuclei to move significantly impulsively excites the molecule to a new nonequilibrium configuration. This results in a nearly vertical promotion of localized material wave packets onto the excited potential surface. The subsequent evolution of this wave packet probed with a pulse of similar duration fully reveals the time course of the excited ensemble, from initial ground state geometry to the final products. Another equally important consequence of impulsive excitation is the buildup of ground-state vibrational coherences through Raman processes. Visualization of these vibrational coherences has become a powerful tool for studying vibrational dynamics in a wide range of molecular systems of varying complexity.[1−12]

Here we report the first observations of vibrational coherences in leghemoglobin (Lba) and make a comparison with the widely studied system, myoglobin (Mb). Hemeproteins play an essential role in a wide variety of physiological functions by their capacity to bind and release external ligands or by their redox properties or both. The heme group (active site) is a planar chromophore containing iron, which is bound to the proximal histidine as the sole covalent link to the protein in Mb. Myoglobin is widely used as a model system for understanding the structural and biophysical mechanisms that govern ligand binding in heme proteins. However, attempts to extrapolate the properties of Mb to a host of other newly discovered hemoglobins have revealed some common features but many differences. This calls for developing model systems based on other heme proteins that could supplement the existing Mb model system in predicting the diverse functional mechanisms of a variety of hemoglobins. Recent studies have shown that leghemoglobin can serve such a purpose.[13−16] Leghemoglobins are small, monomeric heme proteins found in root nodules of leguminous plants where they play an important role in symbiotic nitrogen fixation.[13] They seem to have a ligand binding mechanism distinct from myoglobins and also show many differences in how their distal pocket influences their geminate recombination kinetics.[14−16]

Coherent vibrational oscillations are observed in unligated Lba upon excitation with an ultrashort laser pulse centered on its respective Soret band maximum. The laser field driven oscillations and the parameters associated with them, the amplitudes and phases, are compared with those of unligated Mb. In particular we focus our attention on the iron−histidine (Fe−His) stretching mode at 220 cm^{-1} for Mb and Lba.

Materials and Methods

Proteins. Horse heart myoglobin was purchased from Sigma and used as received. The preparation of Lba is described elsewhere.[16] All the proteins were dissolved in 0.1 M phosphate buffer and then reduced with sodium dithionite to obtain the deligated Fe(II) species.

Apparatus and Measurements. The laser source was a homemade Ti-Sapphire laser (based on the Kapetyn−Murnane design[17]) tunable from 780 to 900 nm with a repetition rate of 82 MHz. Tunability was achieved by translating a slit across the beam. The fundamental was chirp-compensated by a pair of SF10 prisms. The autocorrelation of these pulses was ∼30 fs when measured over the range 810−870 nm. The fundamental was frequency doubled, using a 0.4-mm BBO crystal. The resulting blue pulses had a central wavelength ranging from 405 to 435 nm. These pulses were compressed by a pair of fused silica prisms to compensate for chirp arising from the crystal and other associated optics. The full-width at half-maximum (fwhm) of the blue pulse spectrum was 6 nm when centered at 434 and 428 nm. The pulse width was determined by fitting the rising part of the bleach (which is instantaneous) of the Soret band of the proteins in a one-color pump−probe experiment. Because there was no coherence artifact at time zero, fitting the rise of the bleach provided a good estimate of the pulse width, for which the assumption of a Gaussian shape yields a fwhm of 50 fs. Its time-bandwidth product was 0.48 (at 434 nm) and 0.49 (at 428 nm). The actual value is 0.44 for a transform-limited Gausssian pulse.

Transient Absorption Spectrometer and Data Collection. The central wavelengths (which correspond to the Soret band

* Author to whom correspondence should be addressed.
[†] Department of Chemistry.
[‡] Department of Biochemistry, Biophysics, and Molecular Biology.

10.1021/jp034828u CCC: $25.00 © 2003 American Chemical Society
Published on Web 08/19/2003

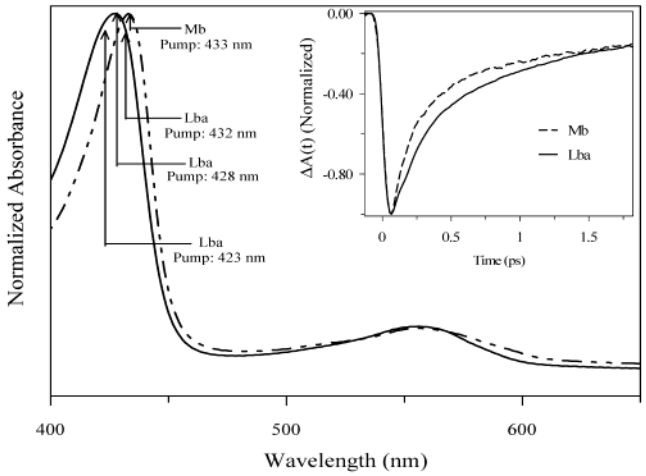

Figure 1. Absorption spectra of unligated myoglobin (dashed) and unligated leghemoglobin (solid) normalized at their respective Soret peaks. The arrows denote the pump wavelengths employed in the coherence experiments. The insert presents the transient absorbance traces of unligated myoglobin (dashed line, pumped and probed at 433 nm) and unligated leghemoglobin (solid line, pumped and probed at 428 nm).

maxima) used for the pump−probe spectroscopy of the proteins are 434 nm for Mb and 428 nm for Lba. The average blue power at the sample is less than 20 mW, which corresponds to about 0.25 nJ per pulse pair. A mechanical chopper modulated the pump beam at 2.3 kHz. The probe beam is passed through an optical delay line. A motorized translation stage (Newport corporation, 3.3-fs/step resolution) controls the pump−probe time delay. The polarization of the pump and probe beams were parallel and focused into the sample with 15- and 10-cm lenses, respectively. The transmitted probe beam was passed through a monochromator (resolution 0.5 nm) and the differential transmittance was detected with a photodiode lock-in amplifier (Stanford SR 810) combination. The time constant for the lock-in was set to 0.3 s, and the dwell time for each time step was set to 1 s to allow for the leveling off of the RC time constant. For each time step, 10 readings from the lock-in were averaged and stored. A total of 150 time steps (each 13.2 fs) were obtained for a single scan, resulting in a 1.98-ps full-scale time window. Each data set consisted of 40−60 scans. The absorption spectra of the samples were checked periodically to ensure sample integrity. The concentrations were adjusted to have an OD of 0.5−0.7 at the maximum of their Soret peak in a rotating cell (1300 rpm) of 0.75-mm path length.

Data Analysis. The transient absorbance data were fit in one of two ways. The first method was by a standard iterative procedure, where the fitting function was

$$\Delta A(t) = \sum A_i \exp(-t/\tau_i) + \text{constant term}$$

where A_i and τ_i are the preexponential factors and time constants, respectively. For Mb the data were well fit to two exponentials, both corresponding to a bleach. For Lba, however, depending upon probe wavelength, the fit can be described as a combination of bleach and induced absorbance. The second method employed a linear predictive singular value decomposition (LPSVD) algorithm, where the fitting function was

$$\Delta A(t) = \sum A_i \cos(\omega_i t - \phi_i) \exp(-t/\tau_i)$$

where A_i , ω_i, ϕ_i, and τ_i denote the amplitudes, frequencies, phases, and time constants (or damping constants), respectively.

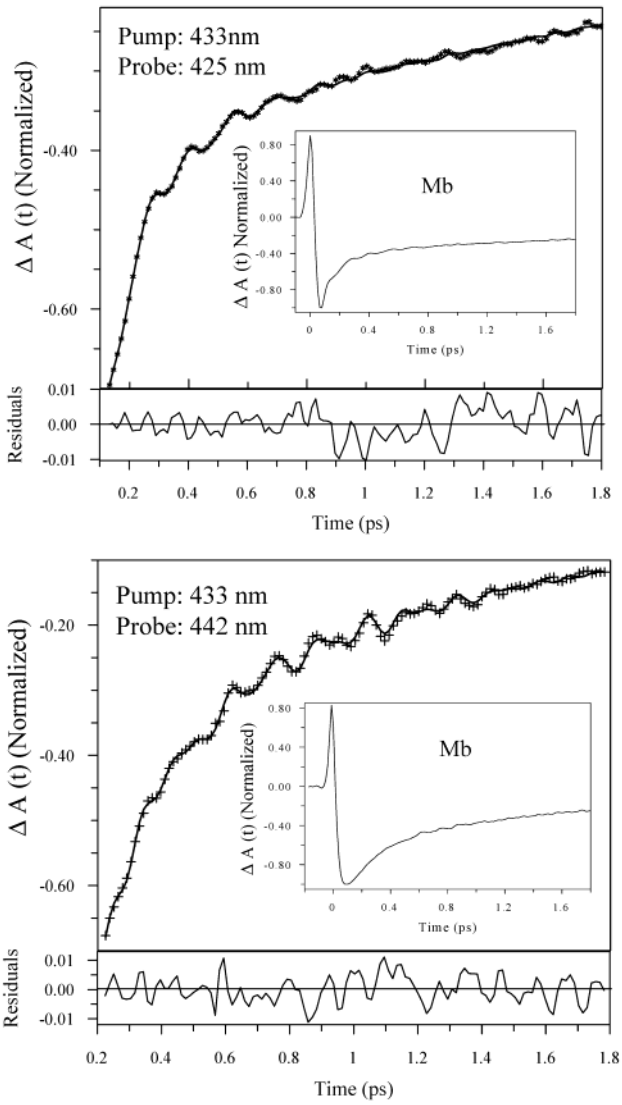

Figure 2. Oscillatory traces for unligated myoglobin pumped at 433 nm and probed at 425 (upper panel) and 442 nm (lower panel). The crosses represent the data; the solid line represents the LPSVD fit. The residuals for the fits are given below the main curve. The inserts present the entire kinetic trace.

For monotonic (i.e., nonoscillatory) decays the frequency is zero and the phase is either 0 or 180° depending upon the sign of the signal (i.e., bleach or absorbance).

The vibrational spectrum is obtained by either Fourier transforming the residuals generated by the iterative fitting procedure or directly from the parameters of the LPSVD fit. We observe that the spectra generated from the LPSVD parameters are more reproducible: when comparing a set of the same transients, the LPSVD procedure consistently gives similar spectra.

Before the data were fit with the LPSVD algorithm, the chirp rate associated with the dispersed detection technique was determined as follows. A series of Mb transients was obtained by pumping at 434 nm and probing from 424 to 444 nm with an interval of 1 nm. Due to the chirp, the time zero for each trace at each wavelength shifted as the probe was tuned from blue to red. The rate of this shift was found to be 3.5 fs/nm. The LPSVD fit begins where the oscillations start. The dead time (time difference between the time zero and the time where oscillation starts) was corrected by incorporating the chirp rate. Each data set typically consisted of about 120−130 points. The

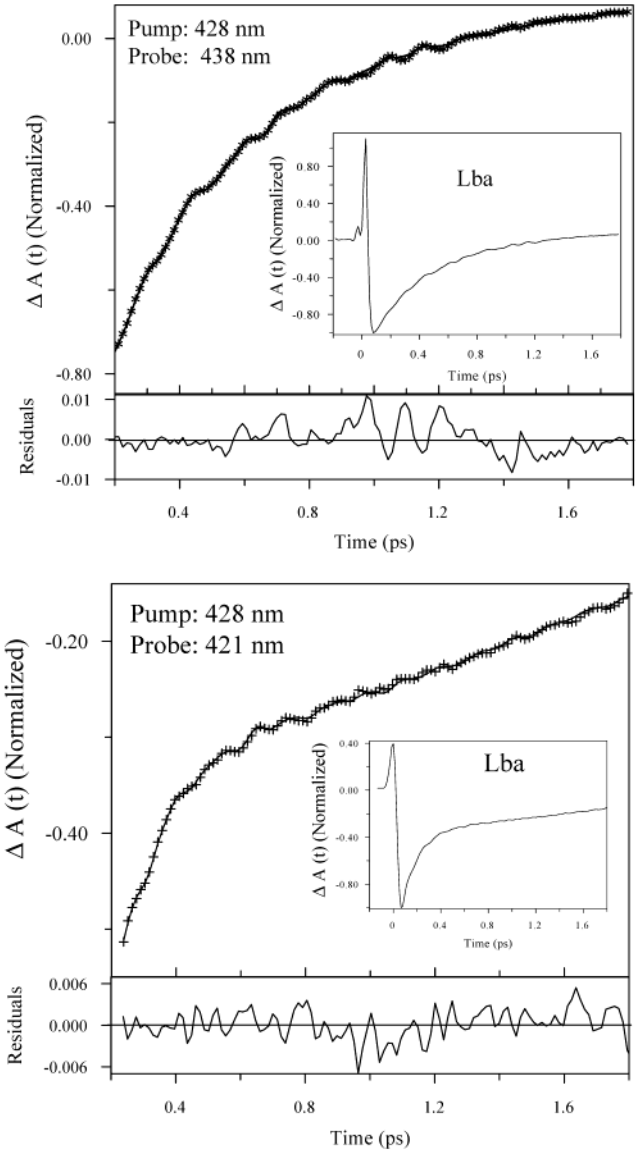

Figure 3. Oscillatory traces for unligated leghemoglobin pumped at 428 nm and probed at 438 (upper panel) and 421 nm (lower panel). The crosses represent the data; the solid line represents the LPSVD fit. The residuals for the fits are given below the main curve. The inserts present the entire kinetic trace.

fitted parameters consisted of two monotonic decays (having zero frequency) and damped oscillations with their amplitudes damping constants and frequency. To generate the power spectrum, the monotonic decay parameters were first removed from the fitted LPSVD parameters. The remaining parameters were used to generate the damped oscillatory signal consisting of different frequencies and corresponding amplitudes. An additional 400 data points (having a value of 0) were added so that the typical data set consisted of about 530 points. This was done so as to increase the resolution of the Fourier transformed spectra. The Fourier transform of this damped oscillatory signal yielded vibrational spectra having a resolution of 5 cm^{-1}. All the spectra displayed are power spectra, normalized to unity at the maximum.

Results

The absorption spectra of the proteins are given in Figure 1. The Soret band absorption maxima for Mb and Lba are 433 and 428 nm, respectively. The inset to the figure presents the transient absorbance traces when pumping and probing the Soret band. For Mb and Lba, the bleach is fully developed within the exciting laser pulse duration and then recovers with two exponential components (∼0.3 and ∼3 ps).

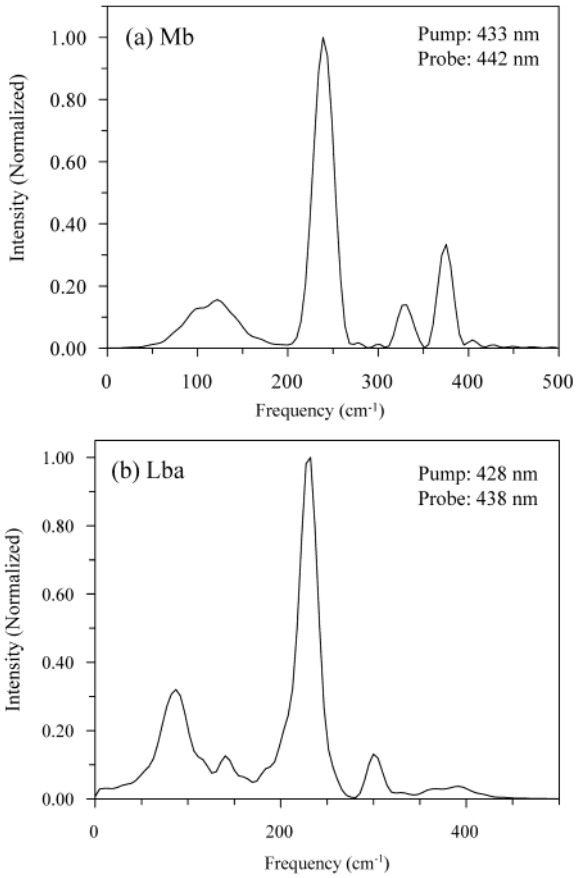

Figure 4. Normalized Fourier transformed power spectra for (a) Mb (λ_{pump} = 433 nm; λ_{probe} = 442 nm) and (b) Lba (λ_{pump} = 428 nm; λ_{probe} = 438 nm).

Since the pump is centered at the maximum of the Soret band, the ground state wave packet initially formed is at the center of the well. Here, the wave packet has maximum momentum, and at the inner and outer turning points, its momentum approaches zero. Consequently when probed at the center of the well, the effective interaction between the wave packet and the probe will be a minimum, and when probed at the turning points, the interaction will be a maximum. As the detuning between the pump and probe increases, the oscillatory components become progressively more visible owing to the increasing interaction of the probe and the wave packet.

Two typical kinetic traces for Mb are shown in Figure 2, where the probe is detuned 9 nm to the red and 8 nm to the blue, with respect to the pump. The oscillatory nature of the curves is clearly visible and damps out at ∼1.8 ps. Figure 3 presents the traces for Lba, where the probe is detuned 10 nm to the red and 7 nm to the blue, with respect to the pump. When the probe is detuned 10 nm to the red it is evident that the signal crosses zero indicating the presence of an absorbing species. The amplitude of oscillation in Lba is less than that in Mb.

The Fourier transformed power spectra for Mb and Lba are presented in Figure 4. Both proteins have low-frequency peaks below or near 100 cm^{-1}. The spectra of Mb and Lba are dominated by the Fe−His stretch at ∼220 cm^{-1}. The relative change of the phase of this mode, as the probe is tuned from

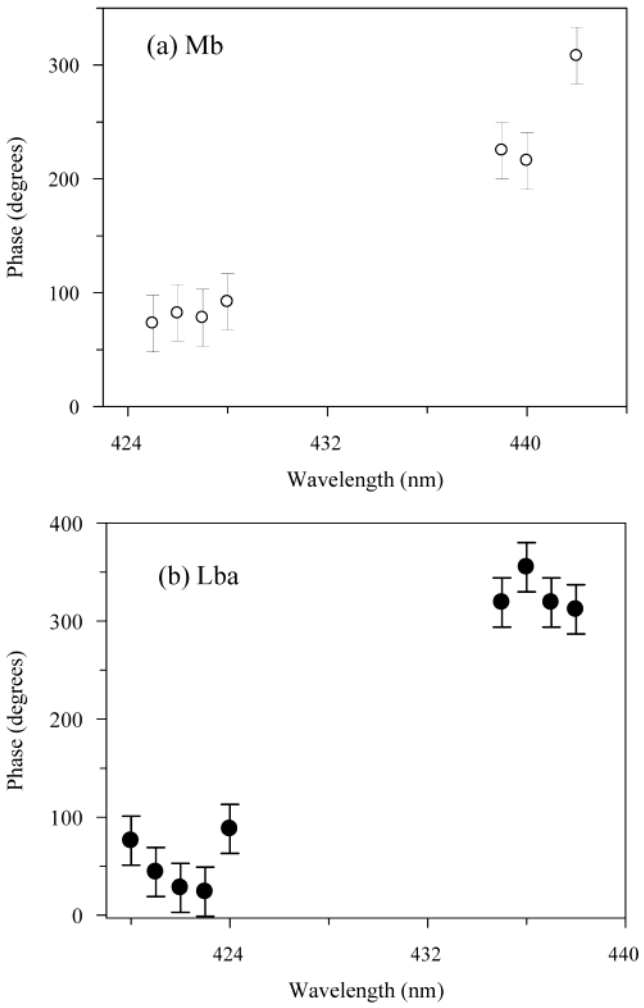

Figure 5. Phase plot for the Fe−His 220-cm^{-1} mode for (a) unligated myoglobin and (b) unligated leghemoglobin as the probe is detuned from blue to red. The phase is obtained from the LPSVD analysis, and there is a maximum of $\pm\pi/4$ error associated with it.

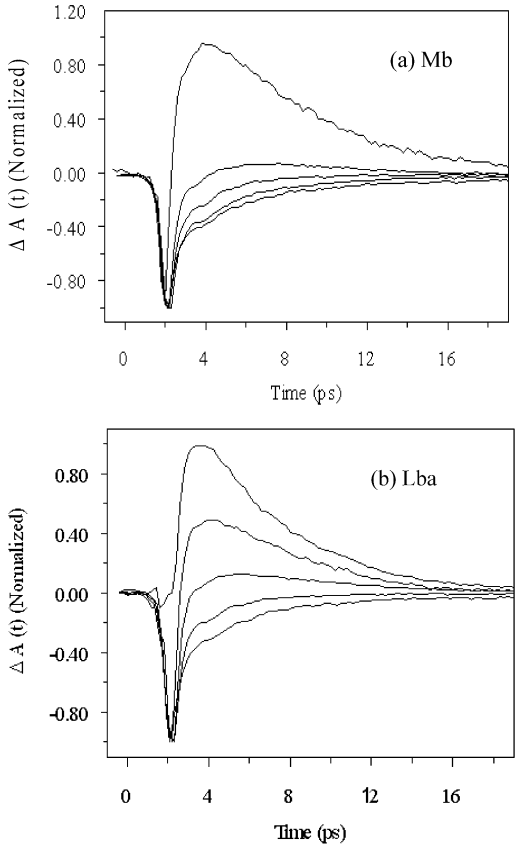

Figure 6. The evolution of the transients pumped at the Soret band. (a) In unligated myoglobin, from bottom to top the probe wavelengths are 426, 430, 435, 438, and 442 nm. (b) In unligated leghemoglobin, from bottom to top the probe wavelengths are 422, 430, 435, 438, and 442 nm.

blue to red, is shown in Figure 5 for Mb and Lba. For Mb, the phase change is $\sim\pi$; for Lb, it is slightly greater than π.

We have performed a two-color pump−probe experiment on Mb and Lba using a 407-nm pump and a white light continuum as probe (Figure 6). For unligated myoglobin, the transients change sign at a probe wavelength of ∼438 nm, and become fully dominated by an absorptive signal at ∼450 nm (data not shown). For Lba the transients start to change their sign at a probe wavelength of ∼435 nm, and are completely dominated by an absorptive signal from probe wavelengths of 440 nm and above.

Discussion

Vibrational coherences can arise in different ways depending on the system. For example, for ligated proteins coherences may be reaction driven.[4,5,11,12] For nonphotodissociable systems, the coherence can be generated by the pump pulse creating wave packets in the excited state and by impulsive Raman scattering creating wave packets in the ground state. These latter processes are typically referred to as field-driven and are the ones responsible for the coherences generated in the unligated proteins investigated here.

An ongoing question that arises in the study of hemeprotein dynamics is the relative importance of excited and ground states. In general, upon optical excitation of unligated hemes two transients are observed, one with a time constant of ∼0.3 ps, another with a time constant of 2−5 ps.[18] It was originally argued that both of these transients correspond to the decay of excited states.[11,18] Subsequently, however, this interpretation has been questioned and the 0.3-ps component has been attributed to internal conversion to the ground state. The longer picosecond component has been attributed to vibrational cooling of the hot ground-state heme generated by the 0.3-ps process.[19,20] In the femtosecond coherence experiments of Champion and co-workers, it has been a fundamental assumption that excited-state population does not contribute to the coherence signal.[4,5] On the other hand, Vos et al.[11] have argued, based on experiments in which the Q-band is excited, that excited-state processes must be taken into account for a proper and complete analysis of hemeprotein vibrational dynamics. In the following discussion, we consider the possibility of rationalizing the leghemoglobin data in terms of excited-state coherences.

The change in phase of a particular vibration when probing in blue and in red gives us important information about the relative displacement of the ground- and excited-state energy surfaces.[10] The presence of excited states is suggested by the kinetic traces in Figure 3. In those where the probe is detuned to the red of the pump, the signal changes sign, from bleach to absorbance. In analyzing the phase changes associated with Lba, we consider the possibility of contributions from excited states in order to show that an interplay between the ground- and excited-state vibrational coherences can account for the observations in Mb and Lba. In the case of deligated Mb, assuming that the Fe−His bond is contracted upon Soret excitation,[21] the

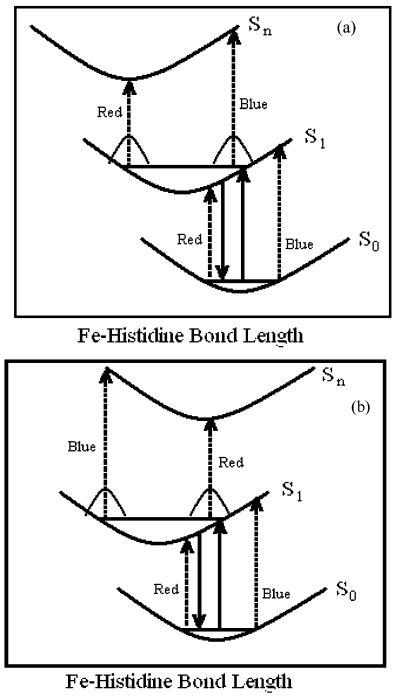

Figure 7. A slice of the potential energy surface along the Fe−His bond. The solid arrows indicate the interaction with the pump and the dashed arrows indicate the interaction with the probe. The designation S_1 in the figure should not be taken in an absolute sense because we are pumping in the Soret band and not the Q-band, which is the lowest lying excited state. Our analysis has not specifically taken into account the presence of the Q-band, although excited state absorption from the Q-band to a higher lying state may similarly complicate the photophysics. Finally, the disposition of the potential energy surfaces in this figure suggests that two-phase jumps might be observed in the data. Unfortunately, there is a large gap in the phase plots in Figure 5 owing to reduced signal and this phenomenon could not be investigated.

excited-state surface will be shifted left with respect to that of the ground state. We assume that this is the case for both proteins.

In Figure 7,we depict a situation where the $S_1 \rightarrow S_n$ transition (excited-state absorption) is also probed along with the $S_0 \rightarrow S_1$ transition (ground-state bleach). Three potential energy surfaces are involved, the ground-state S_0, the first excited-state S_1, and a higher lying state S_n, which is populated by the probe pulse. The surfaces correspond to the 220-cm^{-1} mode. In both panels a and b of Figure 7, the S_1 surface is displaced to the left of S_0 by an arbitrary amount (following the assumption that the Fe−His bond contracts upon Soret excitation[5,21]). In Figure 7a, the S_n surface is displaced to the left of S_1 by an equivalent amount. In Figure 7b, it is not displaced with respect to S_0. Initially the pump pulse (upward pointing thick arrow) launches a wave packet at S_1. After that, interaction with a second pump pulse (downward pointing thick arrow) creates a wave packet, which we depict at the inner turning point of S_0 . The chirp on the pump pulse may also affect the relative densities of the wave packets created in the ground and excited state.[22] In our case, however, the chirp on the pump pulse is not sufficiently severe to produce this effect (see above). For the $S_0 \rightarrow S_1$ transition, probing at red (i.e., at the inner turning point) produces a phase of zero in absorbance units. (In transmission, the phase is π. Note that the data presented in much of the literature[4,5] are given in transmission.) Probing in the blue, i.e., the outer turning point, will give a phase of π. Thus when we are exclusively probing the bleach, we will always see a zero to π phase change in going from red to blue probe wavelengths.

Probing the $S_1 \rightarrow S_n$ transition (i.e., absorbance by a potentially excited heme) gives a different phase relationship depending upon the relative displacements between the S_1 and S_n surfaces. Figure 7a,b depicts the two extreme cases. In Figure 7a, the phase is zero when probed in the blue and π when probed in the red. For Figure 7b, this is reversed: the phase is zero in the red and π in the blue. For situations where there is a mixture of bleach and absorption in the kinetics, depending upon the position of the S_n surface, intensities of oscillations will change significantly. For example, in the case of the situation depicted in Figure 7a, the phase relationships in the bleach and absorbance are opposite. Since bleach and absorption are signals of opposite signs, here the total signal will have a higher oscillation amplitude and the same phase change in going from blue to red. In Figure 7b, the situation is opposite. Here both bleach and absorbance have a similar phase relationship. Thus here the total signal will have a reduced oscillation amplitude; however, the phase change in going from blue to red will be the same as in the earlier case.

In the case of unligated Mb, our results (Figure 5a) indicate that there is a $\sim\pi$ phase change associated with probing at blue and red wavelengths. From the traces in Figure 2 we see that there is no sign change associated either in the red or blue probe wavelengths. Thus in deoxy-Mb the ground-state contribution to the vibrational coherence is the dominant factor. As evident from Figure 3, for the case of deoxy-Lba the oscillatory amplitude is much reduced compared to that for Mb, and the phase change is somewhat greater than π. Considering this, Lba seems to resemble the situation in Figure 7b. Displacement of S_n toward the right with respect to S_1 decreases the amplitude of the oscillations.

While this model does rationalize the differences in the Mb and the Lba signals in terms of excited states and does seem to support the argument of Vos et al.,[11] two points must be taken into account. First, it is not obvious that the excited-state surfaces should be displaced differently for Mb and Lba, as is required in the model presented in Figure 7. Second, it is important to note that these experiments are performed by pumping and probing in the Soret region, and that the Soret band of Lba is considerably broadened with respect to that of Mb (Figure 1). If this broadening of the Soret band in Lba can be attributed to an inhomogeneous distribution of heme sites in the larger heme pocket of Lba,[23] then the diminished amplitude of the oscillations observed for Lba (Figure 3) with respect to Mb (Figure 2) may simply be attributed to the simultaneous excitation of these hemes, which causes a partial cancellation of the total observed amplitude.

To test this idea, we investigated the amplitudes of the oscillations as a function of pump wavelength. The traces in Figure 8 indicate that the amplitude of the oscillations is more pronounced when Lba is pumped at 432 nm than at 423 nm, which is consistent with the idea of heterogeneity of the Soret band reducing the amplitude with respect to that observed in Mb: the intensity of the 220-cm^{-1} feature in the power spectrum is diminshed by about a factor of 2 when pumping at 428 nm as opposed to 432 nm. Consequently, the ground-state heterogeneity of Lba is sufficient to rationalize the decreased vibrational amplitude.

Conclusions

We have compared the vibrational dynamics of the unligated monomeric hemeproteins, Mb and Lba, induced by femtosecond optical pulses. The coherent oscillations induced in Lba are lower in amplitude than those in Mb. It is possible to explain

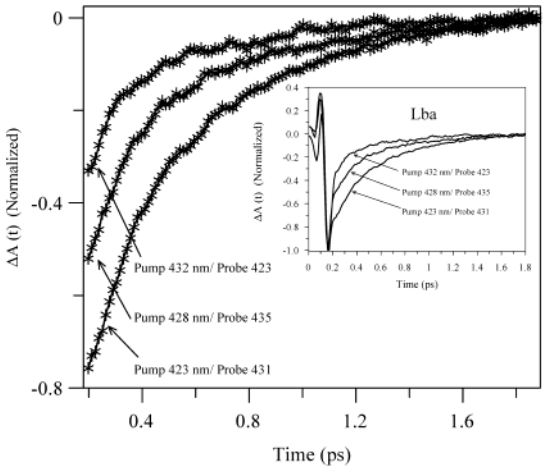

Figure 8. Vibrational dynamics of Lba pumped at, from top to bottom, 432, 428, and 423 nm, respectively. Note that the amplitude of the oscillations is considerably reduced when the sample is excited at 423 nm as opposed to 432 or 428 nm.

this effect by invoking excited states of several picosecond duration, which is currently an object of debate in the literature.[5,11,18−20] An alternative explanation of the reduction in vibrational amplitude is furnished by taking into account the greater breadth of the Soret band in Lba (presumably due to inhomogeneous broadening) with respect to that of Mb. The femtosecond impulsive experiments discussed here are but one example of a wide range of nonlinear optical techniques used to investigate rapid dynamics.[1] Recently Jimenez and Romesberg[20] have used transient grating and three-pulse photon echo peak shift measurements to study related phenomena in cytochrome *c*. Exploitation of such techniques may prove useful in further investigations of Mb and Lba.

Acknowledgment. This work was supported by NSF grant MCB-0077890 to M.S.H. and J.W.P. Professor G. Millhauser graciously provided the LPSVD program. We thank Dr. Marten Vos for helpful conversations.

References and Notes

(1) Mukamel, S. *Principles of Nonlinear Optical Spectroscopy*; Oxford University Press: New York, 1995.

(2) Dexheimer, S. L.; Wang, Q.; Peteanu, L. A.; Pollard, W. T.; Mathies, R. A.; Shank, C. V. *Chem. Phys. Lett.* **1992**, *188*, 61.

(3) Pollard, W. T.; Mathies, R. A. *Annu. Rev. Phys. Chem.* **1992**, *43*, 497.

(4) Zhu, L.; Sage, J. T.; Champion, P. M. *Science* **1994**, *266*, 629.

(5) Rosca, F.; Kumar, A. T. N.; Ye, X.; Sjodin, T.; Demidov, A. A.; Champion, P. M. *J. Phys. Chem. A* **2000**, *104*, 4280.

(6) Vos, M. H.; Martin, J. L. *Biochim. Biophys. Acta* **1999**, *1411*, 1.

(7) Jonas, D. M.; Bradforth, S. E.; Passino, S. A.; Fleming, G. R. *J. Phys. Chem.* **1995**, *99*, 2594.

(8) Vos, M. H.; Rappaport, F.; Lambry, J. C.; Breton, J.; Martin, J.-L. *Nature* **1993**, *363*, 320.

(9) Wang, Q.; Kochendoerfer, G. G.; Schoenlein, R. W.; Verdegem, P. J. E.; Lugtenburg, J.; Mathies, R. A.; Shank, C. V. *J. Phys. Chem.* **1996**, *100*, 17388.

(10) Jonas, D. M.; Fleming, G. R. In *Ultrafast Processes in Chemistry and Photobiology*; El-Sayed, M. A., Tanaka, I., Molin, Y., Eds.; Blackwell Sciences, Ltd.: Oxford, UK, 1995; pp 225−256.

(11) Vos, M. H.; Lambry, J.-C.; Martin, J.-L. *J. Chinese Chem. Soc.* **2000**, *47*, 765.

(12) Liebl, U.; Lipowski, G.; Négrerie, M.; Lambry, J.-C.; Martin, J.-L.; Vos, M. H. *Nature* **1999**, *401*, 181.

(13) Appleby, C. A. *Annu. Rev. Plant Physiol.* **1984**, *35*, 443.

(14) Kundu, S.; Hargrove, M. S. *Proteins: Struct. Func. Gen.* **2003**, *50*, 239.

(15) Chowdury, P. K.; Kundu, S.; Halder, M.; Das, K.; Hargrove, M. S.; Petrich, J. W. Effects of distal pocket mutations on the geminate recombination of NO with leghemoglobin on the picosecond time scale. *J. Phys. Chem.* Accepted for publication.

(16) Kundu, S.; Snyder, B.; Das, K.; Chowdhury, P.; Park, J.; Petrich, J. W.; Hargrove, M. S. *Proteins: Struct. Func. Gen.* **2002**, *46*, 268.

(17) English, D. S.; Zhang, W.; Kraus, G. A.; Petrich, J. W. *J. Am. Chem. Soc.* **1997**, *119*, 2980.

(18) Petrich, J. W.; Poyart, C.; Martin, J. L. *Biochemistry* **1988**, *27*, 4049. Petrich, J. W.; Martin, J. L. *Chem. Phys.* **1989**, *131*, 31.

(19) Kholodenko, Y.; Volk, M.; Gooding, E.; Hochstrasser, R. M. *Chem. Phys.* **2000**, *259*, 71.

(20) Jimenez, R.; Romesberg, F. E. *J. Phys. Chem. B* **2002**, *106*, 9172.

(21) Stavrov, S. S. *Biophys. J.* **1993**, *65*, 1942.

(22) Bardeen, C. J.; Wang, Q.; Shank, C. V. *Phys. Rev. Lett.* **1995**, *75*, 3410.

(23) Hargrove, M. S.; Barry, J. K.; Brucker, E. A.; Berry, M. B.; Phillips, G. N., Jr.; Olson, J. S.; Arredondo-Peter, R.; Dean, J. M.; Klucas, R. V.; Sarath, G. *J. Mol. Biol.* **1997**, *266*, 1032.